J|A|C|S

JOURNAL OF THE AMERICAN CHEMICAL SOCIETY

Article

Interference between the Hydrogen Bonds to the Two Rings of Nicotine

Jrme Graton, Tanja van Mourik, and Sarah L. Price

More About This Article

Additional resources and features associated with this article are available within the HTML version:

- Supporting Information
- Links to the 4 articles that cite this article, as of the time of this article download
- Access to high resolution figures
- Links to articles and content related to this article
- Copyright permission to reproduce figures and/or text from this article

View the Full Text HTML

ACS Publications
High quality. High impact.

Interference between the Hydrogen Bonds to the Two Rings of Nicotine

Jérôme Graton,[†] Tanja van Mourik, and Sarah L. Price*

Contribution from the Centre for Theoretical and Computational Chemistry, University College London, 20 Gordon Street, London WC1H 0AJ, United Kingdom

Received November 4, 2002; E-mail: s.l.price@ucl.ac.uk

Abstract: The biochemical transport and binding of nicotine depends on the hydrogen bonding between water and binding site residues to the pyridine ring and the protonated pyrrolidinium ring. To test the independence of these two moderately separated hydrogen-bonding sites, we have calculated the structures of clusters of protonated nicotine with water and a bicarbonate anion, benzene, indole, or a second water molecule. Unprotonated nicotine–water clusters have also been studied for contrast. The potential energy surfaces are first explored with an intermolecular anisotropic atom–atom model potential. Full geometry optimizations are then carried out using density functional theory to include nonadditive terms in the interaction energies. The presence of the charge on the pyrrolidine nitrogen removes the conventional hydrogen-bonding site on the pyridine ring. The hydrogen-bond ability of this site is nearly recovered when the protonated pyrrolidinium ring is bound to a bicarbonate anion, whereas its interaction with benzene shows a much smaller effect. Indole appears to partially restore the hydrogen-bond ability of the pyridine nitrogen, although indole and benzene both π-bond to the pyrrolidinium ring. A second hydrogen-bonding water produces a significant conformational distortion of the nicotine. This demonstrates the limitations of the conventional qualitative predictions of hydrogen bonding based on the independence of molecular fragments. It also provides benchmarks for the development of atomistic modeling of biochemical systems.

1. Introduction

The hydrogen bond dominates supramolecular chemistry and molecular recognition in biological systems. The characteristic orientation dependence, such as the near linearity of O–H···N[1–3] or N–H···O,[4] is well established, and generally, deviations are only expected when there are multiple donors or acceptors in close proximity giving rise to bifurcated and multi-center hydrogen bonds.[4] Thus, considerable effort has been devoted to understanding hydrogen bonds by experimental and theoretical[5a–c] studies of small model systems. Generally, there is good correspondence between the hydrogen-bonding geometries seen in such "gas-phase" studies of bi-molecular complexes and those seen in crystals and proteins, as derived by statistical database analysis.[6,7] In this paper, we investigate the limitations of

viewing hydrogen-bonding interactions to different functional groups independently. We report density functional theory (DFT) calculations on three molecular clusters comprising of water and other small ligands bound to nicotine, a moderately sized, two-ring biomolecule.

The plant alkaloid, nicotine (Figure 1) is a common drug of abuse that is orally self-administered mainly by the combustion of tobacco products. Cigarettes represent "the most toxic and addictive form of nicotine".[8] The negative effects of nicotine on public health include heart disease, cancer and respiratory disorders.[9,10] However, in addition to its analgesic effects, nicotine has recently been identified to have potentially beneficial effects on neurodegenerative diseases, like Alzheimer's and Parkinson's, on cognitive and attention deficits, Tourette's syndrome and ADHD (attention deficit hyperactivity disorder), anxiety, gastric disorders, and smoking cessation.[11] Nicotine acts

† On leave from Laboratoire de Spectrochimie et Modélisation, Université de Nantes, 2, rue de la Houssinière, BP 92208, 44322 Nantes Cedex 3, France.

(1) Nobeli, I.; Price, S. L.; Lommerse, J. P. M.; Taylor, J. *J. Comput. Chem.* **1997**, *18*, 2060.
(2) Llamas-Saiz, A. L.; Foces-Foces, C.; Mo, O.; Yañez, M.; Elguero, J. *Acta Crystallogr.* **1992**, *B48*, 700.
(3) Ziao, N.; Graton, J.; Laurence, C.; Le Questel, J.-Y. *Acta Crystallogr.* **2001**, *B57*, 850.
(4) (a) Taylor, R.; Kennard, O.; Versichel, W. *J. Am. Chem. Soc.* **1983**, *105*, 5761. (b) Taylor, R.; Kennard, O.; Versichel, W. *J. Am. Chem. Soc.* **1984**, *106*, 244. (c) Taylor, R.; Kennard, O.; Versichel, W. *Acta Crystallogr.* **1984**, *B40*, 280.
(5) (a) Scheiner, S. *Molecular Interactions: From van der Waals to Strongly Bound Complexes*; Wiley: Chichester, 1997. (b) Hadži, D. *Theoretical Treatments of Hydrogen Bonding*; Wiley: Chichester, 1997. (c) Bruno, I. J.; Cole, J. C.; Lommerse, R. S.; Rowland, R. S.; Taylor, R.; Verdonk, M. L. *J. Comput.-Aided Mol. Des.* **1997**, *11*, 525.

(6) Singh, J.; Thornton, J. *Atlas of Protein Side-Chain Interactions*; IRL Press: Oxford, 1992.
(7) Mitchell, J. B. O.; Thornton, J. M.; Singh, J.; Price, S. L. *J. Mol. Biol.* **1992**, *226*, 251.
(8) Henningfield, J. E.; Heishman, S. J. In *Nicotine safety and toxicity*; Benowitz, N. L., Eds.; Oxford: New York, 1998.
(9) Kluger, R. *Ashes to Ashes*; Knopf: New York, 1996.
(10) Sapori, M. In *Neuronal Nicotinic Receptors: Pharmacology and Therapeutic Opportunities*; Arneric, S. P., Brioni, J. D., Eds.; Wiley-Liss: New York, 1998.
(11) See for example: (a) Lloyd, G. K.; Williams, M. *J. Pharm. Exp. Therapeutics* **2000**, *292*, 461. (b) Holladay, M. W.; Dart, M. J.; Lynch, J. K. *J. Med. Chem.* **1997**, *40*, 4169. And references cited. (c) Salin-Pascual, R. J.; Rosas, M.; Jimenezgenchi, A.; Riverameza, B. L.; Delgadoparra, V. *J. Clin. Psychiatry*, **1996**, *57*, 387.
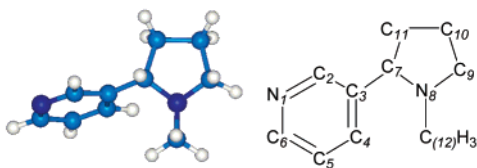
Figure 1. Conformation of neutral and protonated nicotine and numbering scheme.

by binding to the nicotinic acetylcholine receptors (nAChRs).[11b] Several studies[12–15] identify a quaternized amino nitrogen atom and a hydrogen-bond acceptor site as the two key elements of the nicotinic pharmacophore.

Several protonation studies have been carried out on nicotine in both the gas phase[16,17] and in solution.[18,19] In the gas phase, the pyrrolidine and pyridine nitrogen atoms show very similar basic strengths.[16,17] However, a significant difference is observed in water,[18,19] with the first protonation occurring on the pyrrolidine site. Thus, in physiological conditions, with a pK_a value of about 7.74 at 37.2 °C,[20] nicotine is predominantly (about 60%) found in the singly protonated pyrrolidinium form, in addition to the neutral form. Despite the predominance of protonated nicotine (Nic$^+$) in water and the ammonium element in the pharmacophore, the hydrogen-bonding properties have only been studied experimentally for neutral nicotine (Nic^0).[21,22] An early IR study[21] of nicotine with five substituted phenols proposed that the pyridine nitrogen was the only hydrogen-bond acceptor site. Recently, in an extensive theoretical and experimental study using FTIR measurements and ab initio calculations,[22] the authors show that some hydrogen bonding to the pyrrolidine nitrogen is involved, and estimate an approximately 10:1 ratio of pyridine/pyrrolidine complex of nicotine with *p*-fluorophenol.

The original aim of this work was to study the ability of the pyridine nitrogen to act as a hydrogen-bond acceptor in the protonated active form of nicotine (Nic$^+$). The influence of the whole, or partial, neutralization of this charge is also investigated by adding a bicarbonate anion, benzene, indole, or a second water molecule to the Nic$^+$–water complex. These additional molecules interact with the pyrrolidinium site, and have been chosen to represent molecules present in blood or in the active site of nAChRs. Indeed, water and the bicarbonate anion are present in blood, the latter in significant concentration and acting as a p*H*-buffer. The binding of acetylcholine (ACh)[23] and

various quaternary ligands[24] with Acetylcholine Esterase (AChE) probably occurs through cation-π interactions in addition to hydrogen-bond interactions. A synthetic AChR also shows a stabilizing interaction of the quaternary ammonium group of ACh with the electron-rich π-cloud of aromatic rings.[25] Because nicotine is an agonist of ACh, it seemed probable that it also binds to nAChRs through cation-π interactions, though very recent evidence strongly suggests that nicotine has a distinct agonist binding mode.[26,27] Benzene and indole are used to represent the interaction of nicotine with the phenylalanine and tryptophan residues, respectively. The effect of indole is investigated because of the possible presence of tryptophan as cation-π sites,[23] and because it provides a much larger and more intense region of negative electrostatic potential[28] than benzene. However, the increase in size of the clusters involving indole prevents these being studied with ab initio or DFT methods, and so these results had to be extrapolated using the model intermolecular potential method. When the Nic$^+$–water clusters gave unexpected results, calculations were also carried out on Nic^0 and pyridine with water.

The conformation of nicotine (Figure 1) has been well established through experimental[29–36] and theoretical studies.[17,37] The methyl and pyridyl substituents of the pyrrolidine ring prefer the trans configuration with respect to cis-trans isomerization about the C7–N8 bond (Figure 1).[33,35] The pyrrolidine ring adopts an envelope conformation, with different out-of-plane atoms for neutral or protonated nicotine.[17,37] The pyridine and pyrrolidine rings are orientated roughly perpendicular to one another (as indicated by the (C7)H7 atom being approximately in the pyridyl plane) with a sufficiently high barrier to torsion (approximately 110 kJ mol^{-1} for neutral nicotine[17] and 90 kJ mol^{-1} for protonated nicotine[38]) that the molecule is expected to be fairly rigid. This rigid molecule approximation was used for exploring the potential surface, (and as the most reliable feasible calculations for the nicotine-indole-water complexes), using model intermolecular potentials based on an accurate distributed multipole analysis (DMA) model for the dominant electrostatic interaction.

The more reliable calculations of the interaction energies of two and three-body systems involving nicotine were carried out using density functional theory (DFT). DFT methods have been shown to provide an affordable and reliable means of determining the strengths of conventional hydrogen-bonding interactions, yielding dissociation energies in agreement with the best

(12) Beers, W. H.; Reich, E. *Nature* **1970**, *228*, 917.
(13) Sheridan, R. P.; Nilakantan, R.; Scott Dixon, J.; Venkataraghavan, R. *J. Med. Chem.* **1986**, *29*, 899.
(14) Glennon, R. A.; Herndon, J. L.; Dukat, M. *Med. Chem. Res.* **1994**, *4*, 461.
(15) Abreo, M. A.; Lin, N.-H.; Garvey, D. S.; Gunn, D. E.; Hettinger, A.-M.; Wasicak, J. T.; Pavlik, P. A.; Martin, Y. C.; Donnelly Roberts, D. L.; Anderson, D. J.; Sullivan, J. P.; Williams, M.; Arneric, S. P.; Holladay, M. W. *J. Med. Chem.* **1996**, *39*, 817.
(16) Berthelot, M.; Decouzon, M.; Gal, J.-F.; Laurence, C.; Le Questel, J.-Y.; Maria, P.-C.; Tortajada, J. *J. Org. Chem.* **1991**, *56*, 4490.
(17) Graton, J.; Berthelot, M.; Gal, J.-F.; Girard, S.; Laurence, C.; Lebreton, J.; Le Questel, J.-Y.; Maria, P.-C.; Nauš, P. *J. Am. Chem. Soc.* **2002**, *124*, 10 552.
(18) Barlow, R. B.; Hamilton, J. T. *Br. J. Pharmacol. Chemother.* **1962**, *18*, 543.
(19) Fujita, T.; Nakajima, M.; Soeda, Y.; Yamamoto, I. *Pest. Biochem. Phys.* **1971**, *1*, 151.
(20) Calculated with values in Perrin, D. D. *Dissociation Constants of Organic Bases in Aqueous Solution*; Butterworth: London, 1965; supplement 1972.
(21) De Taeye, J.; Zeegers-Huyskens, T. *Bull. Soc. Chim. Belg.* **1987**, *96*, 1.
(22) Graton, J.; Berthelot, M.; Gal, J.-F.; Laurence, C.; Lebreton, J.; Le Questel, J.-Y.; Maria, P.-C.; Robins, R., in preparation.
(23) Sussman, J. L.; Harel, M.; Frolow, F.; Oefner, C.; Goldman, A.; Toker, L.; Silman, I. *Science* **1991**, *253*, 872.

(24) Harel, M.; Schalk, I.; Ehret-Sabatier, L.; Bouet, F.; Goeldner, M.; Hirth, C.; Axelsen, P. H.; Silman, I.; Sussman, J. L. *Proc. Natl. Acad. Sci. U.S.A.* **1993**, *90*, 9031.
(25) Dougherty, D. A.; Stauffer, D. A. *Science* **1990**, *250*, 1558.
(26) Petersson, E. J.; Choi, A.; Dahan, D. S.; Lester, H. A.; Dougherty, D. A. *J. Am. Chem. Soc.* **2002**, *124*, 12 552.
(27) Beene, D. L.; Brandt, G. S.; Zhong, W.; Zacharias, N. M.; Lester, H. A.; Dougherty, D. A. *Biochemistry* **2002**, *41*, 10 262.
(28) Dougherty, D. A. *Science* **1996**, *271*, 163.
(29) Barlow, R. B.; Howard, J. A. K.; Johnson, A. *Acta Crystallogr.* **1986**, *C42*, 853.
(30) Koo, C. H.; Kim. H. S. *Daehan Hwahak Hwoejee* **1965**, *9*, 134.
(31) Chynoweth, K. R.; Ternai, B.; Simeral, L. S.; Maciel, G. E. *Mol. Pharmacol.* **1973**, *9*, 144.
(32) Whidby, J. F.; Seeman, J. I. *J. Org. Chem.* **1976**, *41*, 1585.
(33) Pitner, T. P.; Edwards, W. B.; Bassfield, R. L.; Whidby, J. F. *J. Am. Chem. Soc.* **1978**, *100*, 246.
(34) Seeman, J. I. *Heterocycles* **1984**, *22*, 165.
(35) Whidby, J. F.; Edwards, W. B., III.; Pitner, T. P. *J. Org. Chem.* **1979**, *44*, 794.
(36) Cox, R. H.; Kao, J.; Secor, H. V.; Seeman, J. I. *J. Mol. Struct.* **1986**, *140*, 93.
(37) Elmore, D. E.; Dougherty, D. A. *J. Org. Chem.* **2000**, *65*, 742.
(38) Graton, J.; Berthelot, M.; Laurence, C. unpublished work.

calculations available, in a systematic survey[39] of the energies and structures of 53 hydrogen-bonded complexes of water with various small organic molecules. Hence, we carried out full geometry optimizations at the B3LYP level of theory using the 6-31+G* basis set for our much larger, neutral and charged, organic complexes.

2. Methods

2.1. Model Intermolecular Potential Calculations. The model intermolecular potential calculations were carried out assuming that there is no relaxation of the geometry of each monomer during the complexation. The monomer geometries were kept fixed at the MP2/6-311G(d,p) optimized geometries. To obtain the dissociation energy D_0, the minimum D_e in the potential energy U of the complex is adjusted by the zero-point energy (ZPE) contribution calculated from the harmonic intermolecular vibrational frequencies only. The model potential, dubbed MP2fit/DMA,[40] consists of an atom−atom 6-exp potential to describe the repulsion and dispersion terms, augmented with a DMA[41,42] model to describe the electrostatic interaction (1)

$$U_{MN} = \sum_{a \in M} \sum_{b \in N} A_{\alpha\beta} \exp(-B_{\alpha\beta} R_{ab}) - \frac{C_{\alpha\beta}}{R_{ab}^6} + U^{DMA}(R_{ab}, \Omega_{ab})$$

with

$$A_{\alpha\beta} = (A_{\alpha\alpha} A_{\beta\beta})^{1/2}, B_{\alpha\beta} = \frac{1}{2}(B_{\alpha\alpha} + B_{\beta\beta}), C_{\alpha\beta} = (C_{\alpha\alpha} C_{\beta\beta})^{1/2} \quad (1)$$

The sum runs over the atoms a and b (of type α and β) of each of the molecules M and N, and because all terms are pairwise additive, this can readily be extended to three-molecule complexes. The repulsion and dispersion parameters were empirically fitted to organic crystal structures and heats of sublimation,[43−45] with the oxygen and water hydrogen parameters readjusted[40] to yield good agreement with accurate ab initio data on uracil−water clusters. The DMA electrostatic model includes all terms in the atom−atom multipole expansion up to R_{ab}^{-5}. It uses atomic multipoles up to hexadecapole derived from ab initio wave functions (MP2/6-311G(d,p) for the protonated and neutral nicotine, pyridine, bicarbonate anion, benzene and indole; MP2/6-311++G(2d,2p) for water), computed with the GAUSSIAN 98 package.[46] The program GD-MA[47] was used to compute the DMA models from the Gaussian wave functions, and the model potential calculations on the clusters were carried out with the program ORIENT.[48]

In this potential model, we have neglected the contribution of induction energy, which is expected to be fairly small for neutral species, but more important for interactions of charged

species. The difference between the DFT and model potential energies gives some indication of the effect of this approximation.

The advantage of using the model potential is that we were able to scan thoroughly the potential energy surfaces of the systems studied by performing geometry optimizations from a large number of starting points. The agreement between the model potential and DFT results showed that the model potential would provide worthwhile results on larger systems (protonated nicotine-indole-water) that could not be studied using DFT or MP2 calculations.

2.2. Electronic Structure Calculations. To obtain more accurate structures, full geometry optimizations were carried out at the B3LYP/6-31+G* level, starting from the interaction geometries optimized with the MP2fit/DMA potential. The minima for the other systems, such as Nic^0−water, were also used as additional starting points for a DFT optimization. The geometry optimizations were performed using the GAUSSIAN 98 suite of programs,[46] and MOLDEN[49] was used to visualize and draw the figures. The harmonic vibrational frequencies were calculated for the optimized geometries at the same level of theory to yield estimates of the zero-point vibrational energies (ZPE) corrections to the total energy. All binding energies were corrected for basis set superposition error (BSSE) using the counterpoise procedure.[50,51] The deformation energies of the individual monomers were included in the interaction energies obtained from the full optimizations. Thus, the binding energy of a two-molecule complex AB, $D_e(AB)$, is computed as

$$D_e(AB) = E_{AB}^{\alpha\beta}(AB) - E_A^{\alpha\beta}(AB) - E_B^{\alpha\beta}(AB) + [E_A^{\alpha}(AB) - E_A^{\alpha}(A)] + [E_B^{\beta}(AB) - E_B^{\beta}(B)] \quad (2)$$

The subscripts denote the molecular system considered, whereas the superscripts denote if the energy is computed in the monomer (α or β) or dimer basis set ($\alpha\beta$). The geometry at which the energy is evaluated is indicated in parentheses. Thus, $E_A^{\alpha}(AB)$ is the energy of A at the geometry it has in the complex AB, whereas $E_A^{\alpha}(A)$ is the energy of A at its own equilibrium geometry. The last two terms in brackets are the deformation energies of the fragments A and B, respectively. $D_0(AB)$ is calculated by

$$D_0(AB) = D_e(AB) + E_{ZPE}(AB) - E_{ZPE}(A) - E_{ZPE}(B) \quad (3)$$

where the zero-point energy E_{ZPE} is calculated by the harmonic approximation for all the degrees of freedom. Thus, any changes

(39) Rablen, P. R.; Lockman, J. W.; Jorgensen, W. L. *J. Phys. Chem. A* **1998**, *102*, 3782.
(40) Van Mourik, T.; Price, S. L.; Clary, D. C. *Faraday Discuss.* **2001**, *118*, 95.
(41) Stone, A. J. *Chem. Phys. Lett.* **1981**, *83*, 233.
(42) Stone, A. J.; Alderton, A. *Mol. Phys.* **1985**, *56*, 1047.
(43) Williams, D. E.; Cox, S. R. *Acta Crystallogr.* **1984**, *40B*, 404.
(44) Cox, S. R.; Hsu, L.-Y.; Williams, D. E. *Acta Crystallogr.* **1981**, *37A*, 293.
(45) Mitchell, J. B. O.; Price, S. L. *J. Comput. Chem.* **1990**, *11*, 1217.

(46) Frisch, M. J.; Trucks, G. W.; Schlegel, H. B.; Scuseria, G. E.; Robb, M. A.; Cheeseman, J. R.; Zakrzewski, V. G.; Montgomery, J. A., Jr.; Stratmann, R. E.; Burant, J. C.; Dapprich, S.; Millam, J. M.; Daniels, A. D.; Kudin, K. N.; Strain, M. C.; Farkas, O.; Tomasi, J.; Barone, V.; Cossi, M.; Cammi, R.; Menucci, B.; Pomelli, C.; Adamo, C.; Clifford, S.; Ochterski, J.; Petersson, G. A.; Ayala, P. Y.; Cui, Q.; Morokuma, K.; Malick, D. K.; Rabuck, A. D.; Raghavachari, K.; Foresman, J. B.; Cioslowski, J.; Ortiz, J. V.; Baboul, A. G.; Liu, G.; Liashenko, A.; Piskorz, P.; Komaromi, I.; Gomperts, R.; Martin, R. L.; Fox, D. J.; Keith, T.; Al-Laham, M. A.; Peng, C. Y.; Nanayakkara, A.; Challacombe, M.; Gill, P. M. W.; Johnson, B.; Chen, W.; Wong, M. W.; Andres, J. L.; Gonzalez, C.; Head-Gordon, M.; Replogle, E. S.; Pople, J. A. Gaussian 98, Revision A.9, Gaussian, Inc., Pittsburgh, PA, **1998.**
(47) Stone, A. J. *GDMA: a program for performing Distributed Multipole Analysis of wave functions calculated using the Gaussian program system*, version 1.0, University of Cambridge (UK), 1999.
(48) Stone, A. J.; Dullweber, A.; Engkvist, O.; Fraschini, E.; Hodges, M. P.; Meredith, A. W.; Popelier, P. L. A.; Wales, D. J. *ORIENT version 4.4* University of Cambridge, **2001.**
(49) Schaftenaar, G.; Noordik, J. H. *J. Comput.* − *Aided Mol. Design* **2000**, *14*, 123.
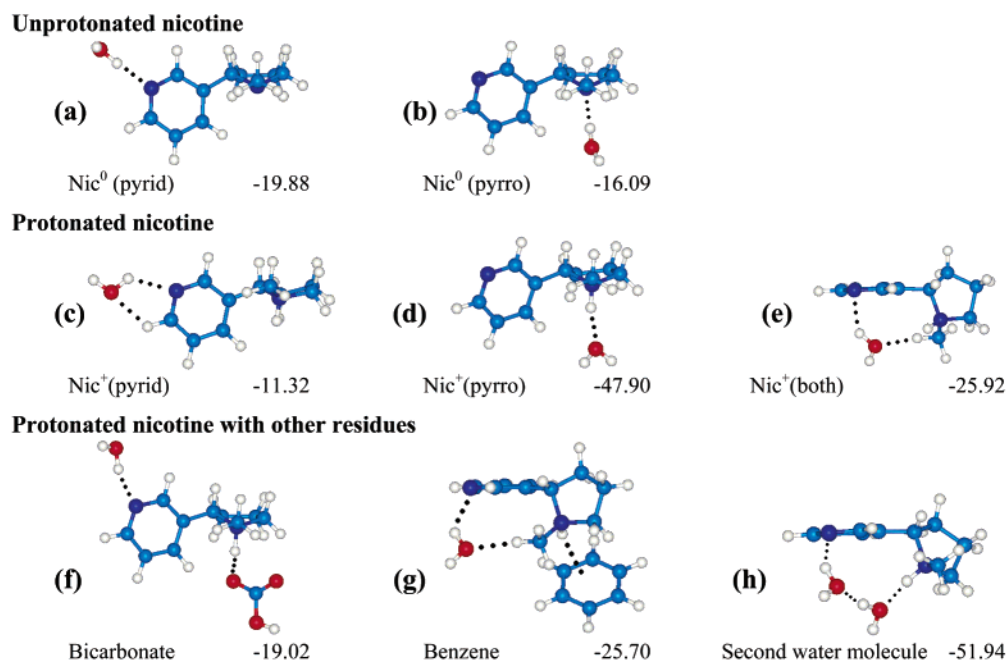
Figure 2. Effect of protonation and third bodies on the water binding sites of nicotine. The B3LYP/6-31+G* optimized structures and the specific interaction energies ΔD_0 (kJ mol^{-1}) from the addition of a water molecule are given.

in the intramolecular vibrations of A and B caused by the formation of the complex are included.

2.3 Comparisons of Effect of Third Body. In estimating the effect of the third molecule, bound to the pyrrolidinium ring, on the strength of the water–nicotine interaction, we require the specific binding energy of one water molecule, ΔD_e (or ΔD_0), to protonated nicotine already bound to, for example, bicarbonate anion. Thus, ΔD_e (or ΔD_0) corresponds simply to the difference between the binding energies of three and two-body systems

$$\Delta D_e = D_e(ABC) - D_e(AB) \tag{4}$$

with a similar formula for ΔD_0. Here, ABC refers to, for example, Nic$^+$–bicarbonate–water and AB to Nic$^+$–bicarbonate.

For the model potential calculations (which employ rigid monomers), this corresponds to the energy gain due to the physical process of adding a water molecule to an existing dimer at its optimal dimer geometry, followed by re-optimization of all the intermolecular parameters to define the trimer geometry. Equation 4 also represents the additional binding energy on addition of a third molecule in DFT calculations in this case where the monomer geometries are allowed to change during the re-optimization of the trimer structure. Since $D_e(AB)$ corresponds to the binding energy of AB at its optimal geometry, the specific binding energy calculated via eq 4 automatically includes the change in dimerization energy [$E_{AB}^{\alpha\beta}(ABC) - E_{AB}^{\alpha\beta}(AB)$], as well as the change in deformation energies of the two monomers in the dimer [$E_A^{\alpha}(ABC) - E_A^{\alpha}(AB)$ and $E_B^{\beta}(ABC) - E_B^{\beta}(AB)$] occurring when the dimer changes from its optimal geometry to the geometry it adopts in the trimer. Both the dimer and trimer D_e energies are free of BSSE, so no additional

BSSE corrections are needed. The computationally demanding three-molecule optimizations were performed on 1.7 to 2.0 GHz Pentium 4 and dual Xeon processors.

3. Results

The structures and corresponding energies of the most important DFT minima found in this study are shown in Figure 2, whereas the DFT and model intermolecular potential energies are given in Tables 1 and 2 for the two-molecule and three-molecule complexes, respectively.

3.1. DFT Minima. The most stable complex of neutral nicotine (Nic^0) with water has a conventional hydrogen bond to the pyridine ring nitrogen (Figure **2a**). Indeed, the steric and electron-withdrawing effects of the pyridine substituent strongly decrease the hydrogen-bond affinity of the amino nitrogen.[22] On the other hand, the effect of the pyrrolidine ring is very small, with the Nic^0–water complex being only about 1 kJ mol^{-1} more stable than pyridine–water (Table 1), with commensurate, insignificant changes to the hydrogen-bond geometry (Table 3). This is consistent with the experimental difference (1.1 kJ mol^{-1}) between pyridine and nicotine complexed to *p*-fluorophenol in carbon tetrachloride.[22]

In contrast, the pyridine hydrogen-bonding site is severely modified in protonated nicotine (Figure **2c**), to give much weaker binding involving an elongated, very nonlinear N···H–O hydrogen bond and a Csp^{2}H···O interaction. This C–H···O interaction is likely to contribute significantly to the stability of this structure, as CH···X (X = N, O) "hydrogen bonds" are recognized to contribute to the stability of many supramolecular structures.[52–55] The loss of the conventional (near-linear) hydrogen bond in Nic$^+$–water was sufficiently unexpected to

(50) Boys, S. F.; Bernardi, F. *Mol. Phys.* **1970**, *19*, 553.
(51) Van Duijneveldt, F. B.; van Duijneveldt-van de Rijdt, J. G. C. M.; van Lenthe, J. H. *Chem. Rev.* **1994**, *94*, 1873.

(52) Taylor, R.; Kennard, O. *J. Am. Chem. Soc.* **1982**, *104*, 5063.
(53) Pedireddi, V. R.; Jones, W.; Chorlton, A. P.; Docherty, R. *Chem. Commun.* **1996**, 997.
(54) Jeffrey, G. A. *J. Mol. Struct.* **1999**, *485–486*, 293.
(55) Desiraju, G. R.; Steiner, T. *The Weak Hydrogen Bond in Structural Chemistry and Biology*; Oxford University Press: Oxford, UK, 1999.

Table 1. Interaction Energies of Two-Molecule Complexes Involving Nicotine, Calculated by DFT and the Model Intermolecular Potential

structure		B3LYP/6-31+G*				MP2fit/DMA		
figure interaction mode[a]	D_e(CP)[b]	Δ(CP)[c]	Δ(ZPE)[d]	D_0		D_e	Δ(ZPE)[d]	D_0
		neutral nicotine−water						
2(a) Nic^0 (pyrid)	−27.62	−3.58	7.74	−19.88		−28.91	7.31	−21.60
2(b) Nic^0 (pyrro)	−26.01	−6.63	9.92	−16.09		−32.58	11.56	−21.02
		protonated nicotine−water						
2(c) Nic$^+$ (pyrid)	−17.95	−2.91	6.63	−11.32		no minimum found		
2(d) Nic$^+$ (pyrro)	−54.88	−6.16	6.98	−47.90		−53.93	6.05	−47.88
2(e) Nic$^+$ (both)	−34.06	−4.04	8.13	−25.92		−30.01	5.59	−24.42
		protonated nicotine−bicarbonate anion						
Nic$^+$ (pyrro)	−472.45	−4.84	−0.34	−472.79		−396.78	3.22	−393.56
		protonated nicotine−benzene						
Nic$^+$ (pyrro)	−29.02	−2.58	2.59	−26.44		−41.51	2.03	−39.48
		protonated nicotine−indole						
Nic$^+$ (pyrro)		DFT calculations not feasible				−59.62	1.95	−57.67
pyridine−water	−26.59	−3.18	7.79	−18.80				

[a] The minima are described by contacts between the nicotine and the second molecule being with the pyridine ring (pyrid), or the pyrrolidinium (or pyrrolidine) ring (pyrro), or the methyl and pyridyl substituents (both). [b] Binding energy corrected from the basis set superposition error (kJ mol^{-1}). [c] Basis set superposition error (kJ mol^{-1}). [d] Zero-Point Vibrational Energy contribution (kJ mol^{-1}).

Table 2. Total Interaction Energies of Protonated Nicotine with Water and a Third Body as Calculated by DFT and a Model Intermolecular Potential

structure		B3LYP/6-31+G*				MP2fit/DMA		
figure interaction mode[a]	D_e(CP)[b]	Δ(CP)[c]	Δ(ZPE)[d]	D_0		D_e	Δ(ZPE)[d]	D_0
		protonated nicotine−water−bicarbonate anion						
2(f) Nic$^+$(pyrid)	−498.82	−8.31	7.20	−491.62		−421.25	10.62	−410.63
Nic$^+$(both)[e]		minimum not found				−415.49	7.98	−407.51
		protonated nicotine−water−benzene						
2(g) Nic$^+$(both)	−60.46	−6.92	10.67	−49.79		−70.93	7.55	−63.38
		protonated nicotine−water−indole						
4(a) Nic$^+$(both)		DFT calculations not feasible				−88.62	6.17	−82.45
4(b) Nic$^+$(pyrid)						−85.83	8.16	−77.67
		protonated nicotine−water−water						
2(h) Nic$^+$(bridge)[f]	−106.49	−14.15	19.84	−86.65		−105.34	19.20	−86.14 (−74.54)
Nic$^+$(both)		Nic$^+$ conformation distorts to min above				−82.54	11.53	−71.00
Nic$^+$(pyrid)		Nic$^+$ conformation distorts to min above				−80.03	13.55	−66.48

[a] The different minima are described by contacts between the nicotine and the water molecule(s) being with the pyridine ring (pyrid), or the pyrrolidinium ring (pyrro), or the methyl and pyridyl substituents (both), or through a chain bridging the two nitrogen atoms (bridge). [b] Binding energy corrected from the basis set superposition error (kJ mol^{-1}). [c] Basis set superposition error (kJ mol^{-1}). [d] Zero-Point Vibrational Energy contribution (kJ mol^{-1}). [e] This minimum has the water in the same position as **2e**, whereas the bicarbonate forms a NH$\cdots$O bond with the pyrrolidinium ring, similar to **2f**. [f] The MP2fit/DMA Nic$^+$(bridge) structure corresponds to the distorted geometry of Nic$^+$ monomer obtained from the DFT optimization. Hence, the D_0 energy allowing for the internal energy change is given in parentheses, as this is the more appropriate value for comparison with the DFT results.

Table 3. Geometries of the O−H$\cdots$N(pyridine) Interactions in Water−Nicotine Complexes[a]

structure	$d_{N1\cdots H}$/Å	$d_{N1\cdots O}$/Å	$\theta_{N1\cdots HO}$/°	$\varphi_{C3C2N1\cdots O}$/°
2(a) neutral nicotine	1.940	2.923	176.9	−175.5
	protonated nicotine			
2(c) isolated	2.267	2.951	126.5	170.4
2(e) isolated	2.415	3.134	130.3	113.2
2(f) +bicarbonate anion	1.952	2.898	160.9	−177.3
2(g) +benzene	2.321	3.067	132.8	116.2
2(h) +water	2.059	2.888	141.1	122.4
4(b) +indole	1.988	2.772	137.6	155.2
pyridine	1.949	2.933	179.5	±174.9

[a] B3LYP/6-31+G* structures are used except for nicotine-indole-water where the MP2fit/DMA potential model structure is used. A positive value of the coplanarity parameter φ means that the water oxygen is on the same side of the pyridine plane as the pyrrolidinium nitrogen.

justify performing careful scans for other possible minima in this region. Thus, we carried out DFT and MP2 geometry optimizations, in addition to the MP2fit/DMA potential calculations, starting from the conventional hydrogen-bonded structure (Figure **2a**) and an alternative structure to Figure **2c** with the

water bent toward the H attached to C2. No additional minima were found, demonstrating that **2c** is indeed the only minimum with water bound to the pyridine nitrogen of Nic$^+$. Thus, the protonation of the pyrrolidine nitrogen has markedly decreased the basicity of the pyridine ring, to reduce the strength of the water-binding energy by almost a factor of 2. The direct effect of protonation on the pyrrolidine ring nitrogen is to change it from being a moderate hydrogen-bond acceptor (Figure **2b**), to a strong hydrogen-bond donor (Figure **2d**). There is a secondary minimum for Nic$^+$−water, involving contact with both the pyridyl and the methyl substituents (Figure **2e**), which is considerably stronger than the interaction of water with just the pyridine ring in either Nic^0 or Nic$^+$, despite neither of the N$\cdots$H−O and Csp^{3}H$\cdots$O interactions being conventional hydrogen bonds. The considerable stability of this structure arises from the water interaction with the charged pyrrolidinium ring through the C$_{12}$(sp^3)H$\cdots$O contact (H$\cdots$O 2.234 Å, C$_{12}\cdots$O 3.318 Å, $\angle$C$_{12}$−H$\cdots$O 170°). The situation is analogous to that found in a study of the linearly C−H$\cdots$O bonded complexes of methane, methylamine or methylammonium and water[56] where there is

Table 4. Specific Pyridine Nitrogen-water Interaction Energies ΔD_e and ΔD_0 in Complexes of Nic$^+$ with Certain Third Molecules Bound to the Pyrrolidinium Nitrogen

structure	B3LYP/6-31+G*				MP2fit/DMA	
figure interaction mode[a]	ΔD_e(CP)[b]	Δ(CP)[c]	Δ(ZPE)[d]	ΔD_0[e]	ΔD_e	ΔD_0[e]
	protonated nicotine−water−bicarbonate anion					
2(f) Nic$^+$ (pyrid)	−26.37	−3.47	7.54	−18.83	−24.47	−17.07
	protonated nicotine−water−benzene					
2(f) Nic$^+$ (pyrid)	−31.44	−4.34	8.08	−23.36	−29.43	−23.90
	protonated nicotine−water−indole					
4(a) Nic$^+$(both)	DFT calculations not feasible				−28.99	−24.77
4(b) Nic$^+$(pyrid)					−26.21	−20.00
	protonated nicotine−water−water					
2(h) Nic$^+$(bridge)[f]	−51.61	−7.99	12.86	−38.75	−51.41	−38.26

[a] The different minima are described by contacts between the nicotine and the water molecule(s) being with the pyridine ring (pyrid), or the methyl and the pyridyl substituents (both), or through a chain bridging the two nitrogen atoms (bridge). [b] Binding energy, calculated from eq 4, corrected for the basis set superposition error (kJ mol^{-1}). [c] Basis set superposition error (kJ mol^{-1}), obtained from the difference between the trimer and the dimer Δ(CP) values. [d] Zero-Point Vibrational Energy contribution (kJ mol^{-1}). [e] Calculated from Equation 4 (kJ mol^{-1}). [f] The MP2fit/DMA Nic$^+$(bridge) structure corresponds to the distorted geometry of Nic$^+$ monomer obtained from the DFT optimization. The specific binding energy ΔD_0 is calculated from the difference of the binding energies found in **2d** and **2h** (see Tables 1 and 2).

a much stronger interaction between water and the protonated structure (−38.9 kJ mol^{-1} compared to −2.6 kJ mol^{-1} for methylamine and −2.2 kJ mol^{-1} for methane) and a shortened equilibrium C···O distance (3.280 Å compared to 3.916 Å for methylamine and 3.863 Å for methane). This may be attributed to the long-range interactions of the charge and the change in polarization of the contact methyl group.

The effect of the introduction of a third molecule on the binding of the water molecule to Nic$^+$ at the distant pyridine ring depends markedly on the third molecule. A bicarbonate anion (HCO$_3^-$) binds strongly to the pyrrolidinium proton (Table 1). A water molecule binds quite strongly to this Nic$^+$−HCO$_3^-$ complex (Table 4), with a very similar energy (∼1 kJ mol^{-1} weaker) as to Nic^0 and in a conventional hydrogen-bonding geometry (Figure **2f**), though somewhat less linear (Table 3) than the pyridine-water hydrogen bond. Thus, the bicarbonate anion has effectively neutralized the protonation of the pyrrolidine ring, in its effect on the distant pyridine binding site.

A benzene molecule π bonds quite strongly to Nic$^+$ through the pyrrolidinium N$^+$−H, effectively blocking the most favorable water−Nic$^+$ binding site. The water binds to the Nic$^+$-benzene complex by a simultaneous interaction with both methyl and pyridyl substituents (Figure **2g**), which is geometrically very similar to the local Nic$^+$−water minimum (Figure **2e**), and only slightly less stable, at −23.48 as opposed to −25.92 kJ mol^{-1}. Thus, the cation-π interaction of Nic$^+$-benzene appears to have little influence on the pyridine nitrogen basicity. No local minimum corresponding to water hydrogen bonding to the pyridine ring (see Figure **2c**) was found. One possible explanation for the absence of such a minimum is that the interaction with benzene may have reduced the barrier between this binding site at the pyridine nitrogen (Figure **2c**) and the more stable structure shown in Figure **2e**. This small effect of the π-bonding to benzene contrasts with the estimated effect of indole as a π-binding residue (section 3.3).

The hydrogen bonding of a water molecule to either ring of Nic$^+$ does not change its conformation, and there is a moderate change when a water molecule is hydrogen bonded to both rings

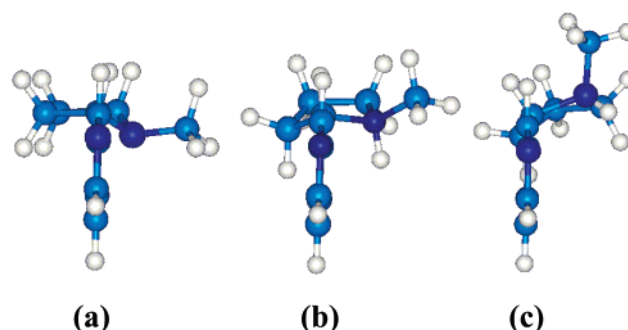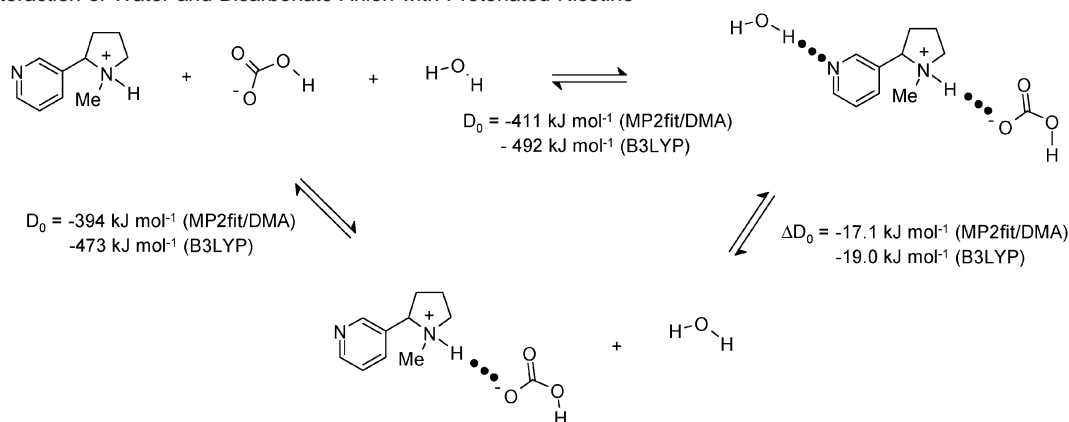(56) Van Mourik, T.; van Duijneveldt, F. B. *J. Mol. Struct. (THEOCHEM)* **1995**, *341*, 63.

Figure 3. Distortion of the protonated nicotine conformation caused by the protonation on the pyrrolidine nitrogen and the binding of two water molecules. **a** uncharged and **b** charged monomers, and **c** when bound to two water molecules as in Figure **2h**, with the water molecules removed for clarity. The pyridyl ring (vertical) is perpendicular to the envelope pyrrolidyl ring with the nitrogen atom out-of-plane, in **a**. The envelope conformation is lost in **b**, and a larger distortion is constrained in **c**.

(Figures **2e** and **2g**). Thus, the C$_2$C$_3$C$_7$H$_7$ torsion angle (which is close to 0 when the two rings are roughly perpendicular) changes from −6° in Nic$^+$ to −16° and −22° in **2e** and **2g**, respectively. However, when a second water molecule is added to the most stable Nic$^+$−water complex, we observe a particularly large distortion of the nicotine conformation (Figure 3) to allow the two water molecules to form a chain bridging the two rings (Figure **2h**). This is the only structure involving an interaction of the water molecules with both the pyridine and the pyrrolidinium nitrogen atoms. In **2h**, the conformation of Nic$^+$ changes by a rotation of 33° between the pyridine and the pyrrolidine rings from the Nic$^+$ monomer geometry (i.e., about twice as large as the rotation observed in **2e** and **2g**), corresponding to a significant intramolecular destabilization of 11.6 kJ mol^{-1}. This is in good agreement with a destabilization of about 10 kJ mol^{-1} for such a rotation in the Nic$^+$ SCF/6-31G(d,p) rotational energy profile.[38] The envelope conformation of the pyrrolidine ring is modified so that the (N8)H atom changes from a gauche to a cis conformation with respect to the C3 atom (the C3C7N8H torsion angle reduces from 47° in Nic$^+$ to 8° in structure **2h**). This conformational change allows the formation of a water bridge linking the two nitrogen atoms of Nic$^+$ through three hydrogen bonds.

Scheme 1 . Interaction of Water and Bicarbonate Anion with Protonated Nicotine

$D_0 = -411$ kJ mol^{-1} (MP2fit/DMA)
-492 kJ mol^{-1} (B3LYP)

$D_0 = -394$ kJ mol^{-1} (MP2fit/DMA)
-473 kJ mol^{-1} (B3LYP)

$\Delta D_0 = -17.1$ kJ mol^{-1} (MP2fit/DMA)
-19.0 kJ mol^{-1} (B3LYP)

3.2. Comparison between DFT and Intermolecular Model Potential Minima.

A comparison of the results obtained from the rigid-body calculations using the intermolecular model potential with those from the full DFT optimizations can be used to assess the effects of neglecting molecular deformation and the approximations in the model potential. This is necessary for assessing whether the model potential calculations are likely to give worthwhile results when applied to larger systems, such as nicotine−indole−water, for which a reliable ab initio or density functional calculation is too expensive.

The intermolecular potential model gives a fairly good qualitative estimate of the geometries of the most significant minima in almost all cases. The intermolecular distances obtained from the model potential calculations agree to within about 10% with the DFT values. The exceptions are the Nic$^+$−(H$_2$O)$_2$ complex, where a significant conformational change of Nic$^+$ during the DFT optimization allowed either of the rigid-model minima to collapse into the chain structure **2h**. This is a clear failure of the rigid-body approximation. However, when this optimized geometry of Nic$^+$ and its corresponding DMA have then been used to reevaluate the interaction energy with the two water molecules using the MP2fit/DMA potential model, the results are in good agreement with the DFT energies. The other exceptions are that the model potential does not give the very shallow local minimum of Nic$^+$−H$_2$O (Figure 2c), and gives an additional local minimum for the Nic$^+$−bicarbonate−water complex. This minimum has the water in the same position as **2e**, whereas the bicarbonate forms a NH···O bond with the pyrrole ring, similar to **2f**. The quantitative agreement between the binding energies is rather more variable. The quantitative agreement between the D_0 values for the Nic$^+$−water complexes conceals more significant differences in the energies of the minima (D_e) and the zero-point energies. This is more apparent in the Nic^0−water results, where the model potential underestimates the difference in the binding energies to the two hydrogen-bonding sites. Nevertheless, if only accuracy of about 1 kcal mol^{-1} is required, these model potential binding energies are acceptable. Considerably large errors occur for the Nic$^+$ complex with the bicarbonate anion or benzene. In the former anion−cation interaction, the underestimate of the binding energy by 80 kJ mol^{-1} (about 16%) is likely to be predominantly due to the lack of induction in the potential model. The interaction energy between Nic$^+$ and benzene is considerably smaller when calculated by DFT than estimated from the model potential. DFT appears unreliable for interactions

that are dominated by the dispersion,[57] such as (He)$_2$, (Ne)$_2$, and (Ar)$_2$, and dispersion is likely to be a major contribution to the Nic$^+$−benzene interaction. On the other hand, the model potential estimates the dispersion contribution by parameters fitted to heats of sublimation. It seems therefore probable that the discrepancy between the Nic$^+$−benzene binding energies is mainly due to errors in the dispersion estimates in the DFT and model potential.

Despite these errors in the energies of some of the two-molecule complexes, there is very good agreement between the two methods for the specific energy ΔD_0 of binding a water molecule to the complex (Table 4). This cancellation of errors is illustrated in Scheme 1. It must be acknowledged that in these three-molecule complexes, the water is separated from the bicarbonate or benzene by the nicotine molecule and so the short-range interactions would be expected to be additive. This additivity cannot be expected for systems where all three molecules are in van der Waals contact with each other. Nevertheless, even for the Nic$^+$−(H$_2$O)$_2$ complex where the two water molecules are linked, the two methods give very similar specific binding energies.

Thus, we would expect the model potential method to give reasonable estimates for the geometries and specific water binding energies ΔD_0 to the pyridine ring for complexes where another molecule was bound to the pyrrolidinium ring of Nic$^+$. This is provided that the rigid-body approximation was reasonable, i.e., the molecule did not have the shape and strength of interaction with water to induce a significant conformational change as in Nic$^+$−(H$_2$O)$_2$. Thus, the model potential approach was used to investigate the effect of indole (as a model for the tryptophan side chain in the nicotinic binding site), as the three-molecule system is too large for DFT calculations to be feasible.

3.3. Effect of Indole on Water Binding Site.

Indole binds more strongly to the pyrrolidinium nitrogen of Nic$^+$ than benzene (Table 1). This is consistent with the electrostatic potential around the π-cloud being more negative for the benzene ring of indole than benzene itself.[30] The model potential finds two minima for the Nic$^+$−indole−water complex (Figure 4). The more stable minimum **4a** has the water in contact with both the pyridyl and methyl substituents of Nic$^+$, and is geometrically very similar to the Nic$^+$−water local minimum **2e** and the Nic$^+$−benzene−water complex **2g**. The model potential estimated specific binding energy for this water

---

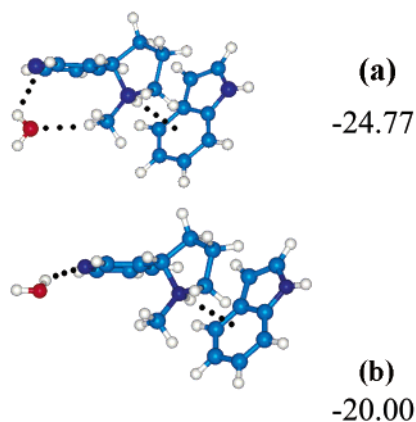(57) Van Mourik, T.; Gdanitz, R. J. *J. Chem. Phys.* **2002**, *116*, 9620.

(a)
-24.77

(b)
-20.00

Figure 4. Geometries of protonated nicotine complexed with indole and water. The specific nicotine-water interaction energies ΔD_0 are given in kJ mol^{-1}, as calculated using the MP2fit/DMA intermolecular potential.

molecule varies by less than 1 kJ mol^{-1} when nothing, benzene or indole are π-bonded to the pyrrolidinium ring. In the secondary minimum **4b**, the indole is found in the same position as in Nic^{+}−indole and in the global Nic^{+}−indole−water minimum **4a**, whereas the water is hydrogen bonded to the pyridine ring. Although the water−pyridine nitrogen hydrogen bond is rather nonlinear (Table 3), and the water molecule is positioned below the plane of the pyridine ring, the specific interaction energy ΔD_0 of −20 kJ mol^{-1} is comparable to the binding energy of water to neutral nicotine. Thus, the interaction of the indole molecule to the pyrrolidinium ring appears to partially restore the hydrogen-bond geometry and strength to that which would be expected from the pyridine ring in isolation. In Nic^{+}−benzene−water, as in the Nic^{+}−water systems, we found no such minimum using either the model potential or the density functional method.

4. Discussion

The most remarkable aspect of the results, shown in Figure 2, is how strongly the hydrogen bonding between water and the pyridine nitrogen is affected by changes in the protonation and interaction of an anion, aromatic compounds or a water molecule to the pyrrolidinium ring. The strong, linear water-pyridine hydrogen bond to Nic^{0} corresponds to the strongly preferred geometry for water molecules bound to a pyridine ring,[5] in the analysis of 342 crystal structures in the Cambridge Structural Database (CSD).[58] The near linearity of the hydrogen bond is consistent with the preference shown in such statistical analyses between aliphatic alcohols and nitrogen acceptors in aromatic heterocycles[1] and for water interacting with various sp^2 nitrogens.[2] Hence, the observation that in the gas phase the pyridine ring of Nic^{+} is no longer a conventional hydrogen-bond acceptor, though it is expected to be one in the nicotinic binding site, demanded investigation.

The resolution of this contradiction is that the presence of a bicarbonate anion, bound to the protonated pyrrolidinium ring, restores the pyridine-water hydrogen bond to its expected strength and geometry. Thus, the addition of certain third bodies, at quite a distance from a hydrogen-bonding site, is shown by these high-level calculations to have a profound effect on the strength and geometry of a traditional hydrogen bond.

A second unexpected result was that the complex with two water molecules (Figure **2h**) induced a significant conformational change in Nic^{+}, far greater than that which would be anticipated from the torsional profile,[17,38] or the geometry of all the other complexes. The large deformation of Nic^{+} (costing 11.6 kJ mol^{-1}) allows two water molecules to link the pyrrolidinium nitrogen to the pyridine nitrogen. The binding energy ($D_0 = -86.7$ kJ mol^{-1}) is about 20 kJ mol^{-1} larger than the sum of the two water hydrogen bonds to pyrrolidinium, estimated from Nic^{+}−water (Figure **2d**) and pyridine (estimated from Nic^{0}−water), which roughly corresponds to the water dimer binding energy.[59−63] Thus, the intra and intermolecular forces are very finely balanced to produce the complex with the unusual conformational change.

The implications of these results on our understanding of the biochemical properties of nicotine in the blood and for its structure in the binding site are to considerably reduce confidence in expectations arising from isolated-molecule and two-molecule studies. The conformation may be considerably changed by the hydration shell or binding site. It is well established that deviations from an ideal hydrogen bond, where the donor heavy atom, the hydrogen, the acceptor lone electron pair and the acceptor all lie in a straight line[64,65] can occur. However, the scatter of hydrogen-bonding geometries around a given functional group found in analyses of protein[5,66−69] or organic crystal databases[4a,4c,70−73] has generally been attributed to the effects of packing of molecules in the vicinity of the hydrogen-bond donor and acceptor. The results of the current study suggest that molecules that are not in van der Waals contact with one or another can have a significant effect on the potential energy surface for the hydrogen bond interaction. However, since the long-range effects from a bicarbonate anion (and, to a lesser extent, from indole) bound to the pyrrolidinium ring, restore the hydrogen-bond geometry and strength to that of the pyridine ring in isolation, the process of considering the two rings in isolation appears to work. However, this cannot be relied upon, since the π-bonding of an indole to the protonated pyrrolidinium is qualitatively different from π−bonding to benzene, and comparable to neutralization by hydrogen bonding to bicarbonate. Moreover, the conformational change of the Nic^{+}− (water)$_2$ system also strongly illustrates the limitations of treating polyfunctional structures to various functional groups independently.

The unexpected results concerning the long-range effects on hydrogen bonding required careful consideration of the reliability of the DFT results. Calculations on adrenaline-water carried out in our laboratory[74] show that B3LYP/6-31+G* gives

(58) Allen, F. H.; Kennard, O. *Chem. Design Automation News* **1993**, *8*, 1.

(59) Xantheas, S. S. *J. Chem. Phys.* **1996**, *104*, 8824.
(60) Feyereisen, M. W.; Feller, D.; Dixon, D. A. *J. Phys. Chem.* **1996**, *100*, 2993.
(61) Halkier, A.; Koch, H.; Jørgensen, P.; Christiansen, O.; Beck Nielsen, I. M.; Helgaker, T. *Theor. Chem. Acc.* **1997**, *97*, 150.
(62) Hobza, P.; Bludský, O.; Suhai, S. *Phys. Chem. Chem. Phys.* **1999**, *1*, 3073.
(63) Torheyden, M.; Jansen, G. *Theor. Chem. Acc.* **2000**, *104*, 370.
(64) Legon, A. C.; Millen, D. J. *Chem. Soc. Rev.* **1987**, *16*, 467.
(65) Legon, A. C.; Millen, D. J. *Acc. Chem. Res.* **1987**, *20*, 39.
(66) Baker, E. N.; Hubbard, R. E. *Prog. Biophys. Mol. Biol.* **1984**, *44*, 97, and references cited.
(67) Thornton, J. M.; MacArthur, M. W.; McDonald, I. K.; Jones, D. T.; Mitchell, J. B. O.; Nandi, C. L.; Price, S. L.; Zvelebil, M. *Philos. Trans. R. Soc. London, Ser. A* **1993**, *345 (1674)*, 113.
(68) McDonald, I. K.; Thornton, J. M. *J. Mol. Biol.* **1994**, *238*, 777.
(69) Klebe, G. *J. Mol. Biol.* **1994**, *237*, 212.
(70) Lommerse, J. P. M.; Price, S. L.; Taylor, R. *J. Comput. Chem.* **1997**, *18*, 757.
(71) Taylor, R.; Kennard, O. *Acc. Chem. Res.* **1984**, *17*, 320.

Table 5. Comparison of Interaction Energies (in kJ mol^{-1}) and Hydrogen-Bond Distances (in Å) Obtained from B3LYP/6-31+G* and MP2/6-31+G* Optimizations

	B3LYP/6-31+G*			MP2/6-31+G*		
structure	D_e(CP)	Δ(CP)	R[a]	D_e(CP)	Δ(CP)	R[a]
Nic^0(pyrid)	−27.62	−3.58	1.94	−26.64	−9.69	1.96
Nic$^+$(pyrid)	−17.95	−2.81	2.27	−20.58	−7.16	2.26
Nic$^+$(pyrro)	−54.88	−6.16	1.86	−59.29	−16.27	1.84
Mepyrro$^+$-benzene[b]	−37.52	−2.05	2.38	−57.67	−20.47	2.20

[a] Nic^0(pyrid) and Nic$^+$(pyrid): the H(water)-N$_1$ distance; Nic$^+$(pyro): the H(water)-N$_8$ distance; Mepyrro$^+$-benzene: the distance from H(water) to the plane of benzene. [b] The hydrogen-bond distance was corrected for BSSE by numerically locating the distance for which the counterpoise-corrected binding energy has its maximum. This correction can be large for π-bonded systems.[76] This numeric re-optimization increased the hydrogen-bond distance by 0.025 (B3LYP) and 0.16 (MP2) Å, and the interaction energy increased by 1.11 (B3LYP) and 2.11 (MP2) kJ mol^{-1} from the minimum found without BSSE correction.
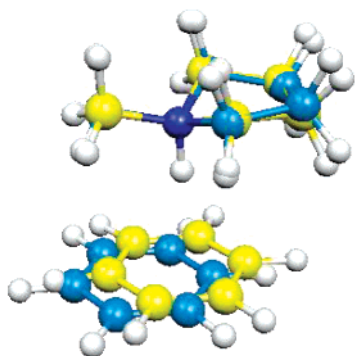

Figure 5. Geometry of *N*-methylpyrrolidinium-benzene, calculated with B3LYP/6-31+G* and MP2/6-31+G*. The B3LYP and MP2 structures are superimposed with the NH bonds in the same place. The geometry with the yellow carbon atoms is the MP2-optimized structure.

interaction energies and geometries in very good agreement with MP2 results, for neutral hydrates containing only σ-type hydrogen-bonding interactions, thus confirming the conclusions of ref 39. To investigate the suitability of DFT for the neutral and protonated systems studied in the current paper, we re-optimized the structures of Nic^0(pyrid) (Figure **2a**), Nic$^+$-(pyrid) (Figure **2c**), and Nic$^+$(pyrro) (Figure **2d**) with an MP2/6-31+G* wave function. Because MP2 optimizations on Nic$^+$-benzene are too computationally demanding, we also optimized the structure of *N*-methylpyrrolidinium-benzene (Mepyrro$^+$-benzene) at the MP2 level to investigate the reliability of DFT for structures that contain π-type interactions. The results are shown in Table 5. DFT gives interaction energies and geometries comparable to MP2 for all structures except Mepyrro$^+$-benzene. However, even in this case, the geometries are quite similar (see Figure 5); with the (N)H atom pointing somewhat more closely to the center of the benzene ring in the MP2 structure. This, in addition to the expectation that the error in the Mepyrro$^+$-benzene interaction energy will cancel (cf. Scheme 1), indicates that the DFT method is adequate for the calculation of the specific binding energies of an additional water, ΔD, for the three-body complexes in this study.

The differences between the three-molecule complexes and what would be extrapolated from two-molecule studies, or models based on the separate rings of nicotine, obviously poses

a challenge to molecular modeling. The changes in hydrogen-bonding acceptor capabilities of the pyridine ring with the nature of the pyrrolidinium interactions clearly require considerable accuracy in the long range interactions. The degree of conformational change induced by two water molecules, where no significant conformational flexibility had been seen in any other complex, shows the challenging requirement that force fields balance the inter and intramolecular interactions accurately. In this work, we used a model intermolecular potential with an unusually accurate anisotropic electrostatic model, though no molecular flexibility or induction energy. This proved to be a useful method for scanning multidimensional potential energy surfaces to locate less obvious low-energy structures as starting points for the more expensive optimizations. The level of agreement between the two methods in estimating interaction energies shows that it gives worthwhile results in cases where high-quality electronic structure calculations are not feasible. The induction energy is clearly significant for the anion−cation interaction energies, though not for semiquantitative structures or for specific binding energies for the introduction of an additional molecule. Thus, the use of a distributed multipole electrostatic model appears to be working as well as found for small molecule hydrogen-bonded complexes[64,75] in predicting hydrogen-bonding contact geometries well, even when there is significant influence from more distant parts of the molecule or supramolecular complex.

5. Conclusions

Our investigations of the hydrogen-bonding ability of the pyridine nitrogen in the active protonated form of nicotine show that it is very dependent on the molecules around the pyrrolidinium ring. The introduction of a charge on the pyrrolidinium nitrogen drastically decreases the hydrogen-bond ability of the nicotine sp^2 nitrogen. This can be restored if the pyrrolidinium ring interacts with a bicarbonate anion, partially restored if it interacts with indole, but is unaffected by interaction with benzene. It appears, from the similarity between the results of the DFT calculations and a model intermolecular potential with an accurate electrostatic potential, that this effect is predominantly due to the modification of the electrostatic potential in the region of the pyridine ring. Since the pyridine nitrogen appears to be a hydrogen-bond acceptor in the nicotinic pharmacophore,[12−15] it seems probable that the residues in the binding site significantly contribute to this hydrogen-bond strength.

A second finding is that it cannot be assumed that the bound conformation of nicotine is similar to the gas-phase conformation, despite the significant torsional barrier. Whether the Nic$^+$−(H$_2$O)$_2$ complex, with the high-energy conformer stabilized by water hydrogen bonds linking the nitrogen atoms in the two rings, would be found in Nic$^+$ aqueous solutions or binding sites is an open question, but there is certainly an unusual balance of molecular geometry, intermolecular and conformational forces producing this structure (Figure **2h**). Thus, density functional calculations on nicotine with small model molecules interacting with the pyridine and pyrrolidinium rings show

(72) Leiserowitz, L.; Tuval, M. *Acta Crystallogr.* **1978**, *B34*, 1230.
(73) Murray-Rust, P.; Glusker, J. P.; *J. Am. Chem. Soc.* **1984**, *106*, 1018.
(74) Van Mourik, T., unpublished.

(75) Buckingham, A. D.; Fowler, P. W.; Stone, A. J. *Int. Rev. Phys. Chem.* **1986**, *5*, 107.
(76) (a) Van Mourik, T.; Price, S. L.; Clary, D. C.; *Chem. Phys. Lett.* **2000**, *331*, 253. (b) Tsui, H. H. Y.; Van Mourik, T., *Chem. Phys. Lett.* **2001**, *350*, 565.

significant interactions between all three molecules, even when there is no contact between the nicotine ligands. This reveals the limitations of experiments and calculations on model systems considering only two molecules, or splitting the biomolecule into molecular fragments, in predicting the behavior of molecules in biochemical environments. However, the increasing feasibility of DFT and correlated ab initio calculations on many body clusters involving larger molecules will provide the opportunity to refine force fields suitable for simulating even larger many-body systems.

Supporting Information Available: Cartesian coordinates of the monomers used and complexes obtained with intermolecular potential model MP2fit/DMA. Cartesian coordinates and electronic energies of the monomers and complexes optimized at the B3LYP/6-31+G(d) level. This material is available free of charge via the Internet at http://pubs.acs.org.

JA029213+